Matrix-Assisted Laser Desorption Ion Trap Mass Spectrometry: Efficient Trapping and Ejection of Ions

Jun Qin and Brian T. Chait

The Rockefeller University, 1230 York Avenue, New York, New York 10021

ANALYTICAL® CHEMISTRY

Reprinted from
Volume 68, Number 13, Pages 2102–2107

Anal. Chem. **1996,** *68,* 2102–2107

Matrix-Assisted Laser Desorption Ion Trap Mass Spectrometry: Efficient Trapping and Ejection of Ions

Jun Qin and Brian T. Chait*

The Rockefeller University, 1230 York Avenue, New York, New York 10021

The present paper explores the coupling of a matrix-assisted laser desorption/ionization (MALDI) ion source with an ion trap mass analyzer, with particular emphasis on the development of methods for improving the efficiency of ion trapping and ejection. A technique is described for directly measuring, for the first time, the trapping efficiency of peptide ions produced in a remote external MALDI ion source. The technique was used to devise an improved scheme for trapping, which yielded efficiencies as high as 39%. An improved understanding of the resonant ejection process led us to a new resonant ejection parameter set that increased the ejection efficiency by 1 order of magnitude over more conventionally used parameter sets and allowed for marked improvements in the mass resolution of ions with *m/z* > 2500. The presently described improvements in the efficiencies of ion trapping and ejection together with improved methods for isolating and fragmenting ions (Qin, J.; Chait, B. T. *Anal. Chem.*, following article in this issue) lay the foundation for highly sensitive MALDI ion trap mass spectrometry of proteins (Qin, J.; et al. *Anal. Chem.* 1996, *68,* 1784–1791).

It has long been recognized that ions can be injected into a quadrupole ion trap mass spectrometer (ITMS) from a remote source or from a boundary of the trap.[1,2] Interest in these methods of ion injection has recently been stimulated by advances in ITMS operation[3,4] and the introduction of effective new ionization sources for biopolymers that use matrix-assisted laser desorption/ionization (MALDI)[5] or electrospray ionization (ESI).[6] The demand for high sensitivity in biological applications requires efficient interfacing of such ionization sources to the mass spectrometer and efficient detection of the trapped ions. In the present paper, we explore the coupling of the MALDI ion source with the ITMS and discuss methods to achieve efficient ion trapping and ejection. For tandem mass spectrometric analysis it is also necessary to isolate and fragment ions of interest effectively. A companion paper[7] describes methods for efficient ion isolation and effective fragmentation.

Ions produced by MALDI have broad energy distributions,[8] which render the ions difficult to trap without significant loss. Two approaches have been adopted to address this issue. The first involves "static trapping" wherein the amplitude of the rf trapping field is held constant during injection and trapping.[3,9–12] With this method, trapping is brought about solely by collisional damping of the kinetic energy of the injected ions to a value that falls within the trapping potential set by the rf field. The efficiency for static trapping is rather poor. The second approach is called "dynamic trapping",[13,14] wherein the amplitude of the rf field is initially set to a low level to permit easy penetration of the rf field by ions injected through the entrance trap electrode; thereafter, the amplitude of the rf field is rapidly ramped to a high level (to provide a high trapping potential) to facilitate trapping before ions have traveled to the opposite electrode and are lost. In this latter case, the dynamically increasing trapping field and collisional damping are responsible for trapping. The efficiency of dynamic trapping is better than that of static trapping, with reported efficiency improvements of 1 order of magnitude for a source positioned at the boundary of the ring electrode ("boundary source").[14] For such a boundary source, synchronization of the laser firing with the rf phase has been reported to either improve trapping[13] or have no effect.[14] There is currently no report of the implementation of dynamic trapping for a remote "external source" and no direct measurement of the trapping efficiency under any conditions.

Once ions are efficiently trapped, it is necessary to detect the trapped ions efficiently. The current method of choice for the detection of high-*m/z* ions (>650) is resonant ejection.[3] It has been recognized through simulations that ion ejection requires a special phase relationship between the resonance ejection supplemental ac field and the driving rf field.[15] When the phase

(1) Schuessler, H. A.; Chun-Sing, O. *Nucl. Instrum. Methods Phys. Res.* **1981,** *186*(1–2), 219–230.
(2) Louris, J. N.; Amy, J. W.; Ridley, T. Y.; Cooks, R. G. *Int. J. Mass Spectrom. Ion Processes* **1989,** *88,* 97–111.
(3) Kaiser, R. E., Jr.; Cooks, R. G.; Stafford, G. C., Jr.; Syka, J. E. P.; Hemberger, P. H. *Int. J. Mass Spectrom. Ion Processes* **1991,** *106,* 79–115.
(4) Schwartz, J. C.; Syka, J. E. P.; Jardine, I. *J. Am. Soc. Mass Spectrom.* **1991,** *2,* 198–204.
(5) Hillenkamp, F.; Karas, M.; Beavis, R. C.; Chait, B. T. *Anal. Chem.* **1991,** *63,* 1193A–1203A.
(6) Fenn, J. B.; Mann, M.; Meng, C. K.; Wong, S. F.; Whitehouse, C. M. *Mass Spectrom. Rev.* **1990,** *9,* 37–70.
(7) Qin, J.; Chait, B. T. *Anal. Chem.* **1996,** *68,* XXXX–XXXX.
(8) (a) Beavis, R. C.; Chait, B. T. *Chem. Phys. Lett.* **1990,** *123,* 1–10. (b) Ens, W.; Mao, F.; Mayer, F.; Standing, K. G. *Rapid Commun. Mass Spectrom.* **1991,** *5,* 117–123. (c) Pan, Y.; Cotter, R. J. *Org. Mass Spectrom.* **1992,** *27,* 3–8.
(9) Chambers, D. M.; Goeringer, D. E.; McLuckey, S. A.; Glish, G. L. *Anal. Chem.* **1992,** *27,* 1151–1152.
(10) Doroshenko, V. M.; Cornish, T. J.; Cotter, R. J. *Rapid Commun. Mass Spectrom.* **1992,** *6,* 753–757.
(11) Jonscher, K.; Currie, G.; McCormack, A. L.; Yates, J. R., III *Rapid Commun. Mass Spectrom.* **1993,** *7,* 20–26.
(12) Schwartz, J. C.; Bier, M. E. *Rapid Commun. Mass Spectrom.* **1993,** *7,* 27–32.
(13) Eiden, G. C.; Cisper, M. E.; Alexander, M. L.; Hemberger, P. H.; Nogar, N. S. *J. AM. Soc. Mass. Spectrom.* **1993,** *4,* 706–709.
(14) Doroshenko, V. M.; Cotter, R. J. *Rapid Commun. Mass Spectrom.* **1993,** *7,* 822–827.

S0003-2700(95)01162-0 CCC: $12.00

difference between the ac and rf fields is random, the appropriate phase difference for ejection may not occur on every ac cycle, and ions will only be ejected on ac cycles when this condition is accidentally satisfied—making efficient ion ejection difficult. To take advantage of ac cycles where the appropriate phase condition is accidentally met, a high ac amplitude is normally used to assist in the ejection of ions. As we will see in the present paper, the use of high ac supplementary fields has its pitfalls, which include inefficient and premature ejection of ions—problems that are especially severe for high m/z species. New strategies are needed to circumvent these problems because the schemes that have been devised for operating the ITMS for the ejection of small ions[3] cannot be directly transferred to the analysis of large peptide ions without careful reevaluation.

In the present paper, we describe a method for direct measurement of the trapping efficiency of ions produced in a remote external MALDI ion source and improved techniques for trapping and ejecting peptide ions.

EXPERIMENTAL SECTION

A full description of the instrument is described in a companion paper.[16] Briefly, the apparatus consists of an external MALDI source, an electrostatic lens, an ion trap, and a channeltron detector with a −10 kV conversion dynode. To improve the efficiency of ion transfer into the ion trap, we replaced the entrance end cap (containing a single hole) with a standard Finnigan ITMS detector end cap (containing seven holes). The rapid ramping of the rf field used in dynamic trapping relies on the inherent time constant of the Finnigan ITMS apparatus, which takes ~170 μs to ramp from zero amplitude to any rf value specified in the control software. The firing of the laser is timed so that ions arrive at the entrance end cap on the rising slope of this fast rf ramp. A custom data system incorporating a LeCroy 9450 digital oscilloscope (LeCroy Corp., Chestnut Ridge, NY) was used for all the present experiments. This data system has the useful property that the oscilloscope can be triggered at an arbitrary time subsequent to the laser desorption event. Thus, we can monitor the fate of ions during the whole scan process of trapping, cooling, isolation, resonant excitation, and resonant ejection. Any ions that exit the detector end cap can be captured by the detector during the complex array of rf scan functions, allowing us to readily monitor the influence of the scan function on the stability of ion trajectories in the trap. The detector ion extraction plate (bias −3 kV) is placed close to the exit end cap (~0.5 cm), so that ions are detected with little delay upon exit from the ion trap. In all the experiments reported here, ions were accelerated to 25 eV for injection and He was used as the buffer gas. A matrix of 2,5-dihydroxybenzoic acid (DHB) was used for MALDI.

RESULTS AND DISCUSSION

Ion Trapping. Figure 1 depicts rf waveforms used in three different trapping schemes. Figure 1a shows the waveform used for static trapping in which the rf amplitude is held constant during ion injection and trapping. We define the time when the packet of ions reaches the entrance end cap as the ion injection time (which has a spread of 15–35 μs for peptides with 500 < m/z <

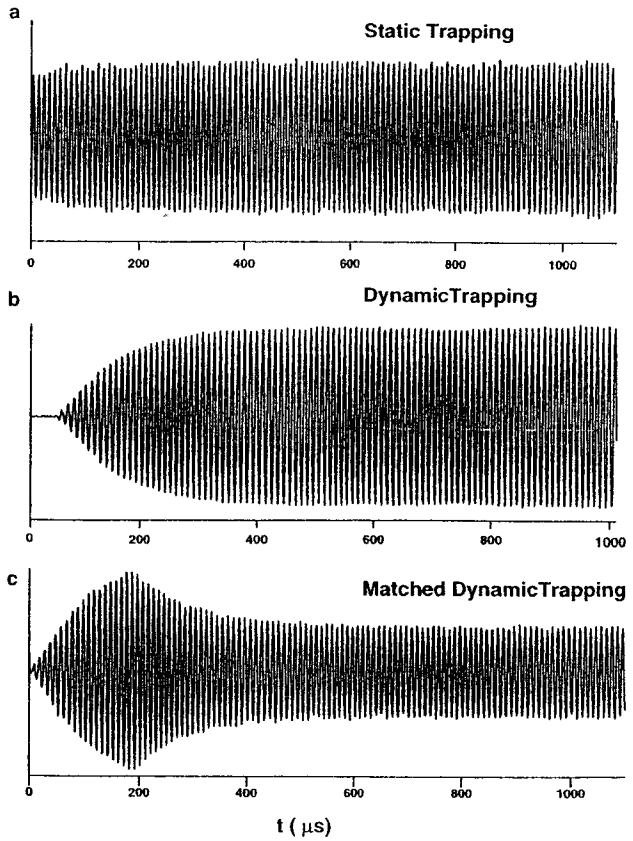

Figure 1. rf waveforms measured using an antenna and recorded by a digital oscilloscope.

6000, under the present experimental conditions), the time after injection until ions are collapsed within the trapping volume as the trapping time (~700 μs), and the time for ions to collapse to the center of the trap as the cooling time (>5 ms). Figure 1b depicts dynamic trapping in which the rf field is ramped rapidly over a period of ~170 μs from zero to an elevated level, which is maintained constant for subsequent trapping and cooling. Ion injection is timed to occur on the rising slope of the rf waveform. Figure 1c is the rf waveform for a method that we term matched dynamic trapping, wherein a rapid down ramp (to a minimum level V_2) is applied subsequent to the up ramp (to a maximum level V_1). After the down ramp, the lower rf level (V_2) is maintained for subsequent cooling. In this trapping scheme, injection is timed to occur on the rising slope of the rf waveform (as in dynamic trapping), with trapping occurring between the rising and the falling slopes.

The shot-to-shot instability of the MALDI ion source makes it difficult to obtain reliable measurements of the trapping efficiency if ion intensities are compared from different laser shots. We, therefore, devised a direct means to determine the absolute trapping efficiency by monitoring both the trapped and untrapped ions from the same laser shot. Because our instrument incorporates semitransparent entrance and exit end cap electrodes (see Experimental Section), ions that are not trapped pass through these electrodes and strike the detector. These untrapped ions arrive at the detector at early times subsequent to the laser pulse (<0.1 ms). Ions that are actively trapped are cooled and then resonantly ejected and detected at much later times (>10 ms). For absolute efficiency measurements, the intensities of the trapped ions are compared to the intensities for the untrapped ions as illustrated in Figure 2. In this example, bombesin ions

(15) Julian, R. K., Jr.; Reiser, H. P.; Cooks, R. G. *Int. J. Mass Spectrom. Ion Processes* **1993**, *123*, 85–96.

(16) Qin, J.; Steenvoorden, R. J. J. M.; Chait, B. T. *Anal. Chem.* **1996**, *68*, 1784–1791.

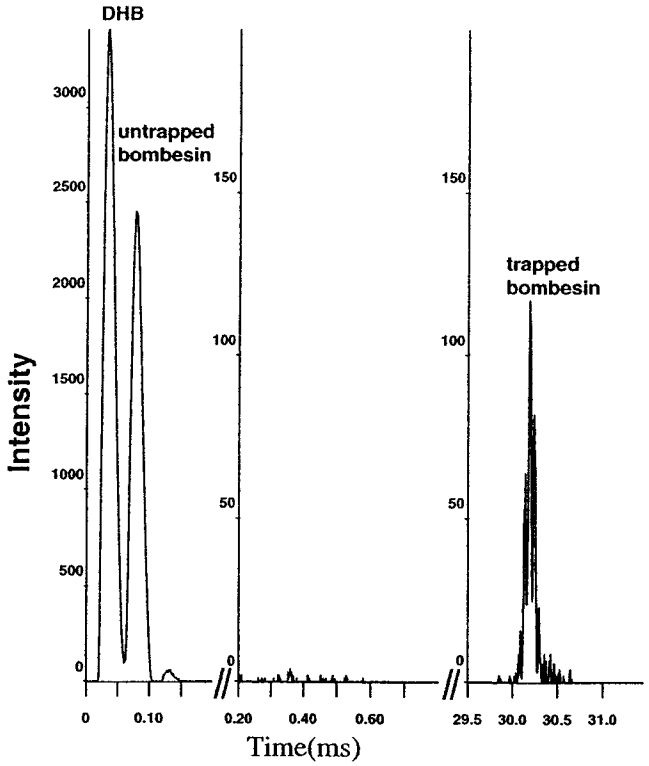

Figure 2. Trapping efficiency measurement in which the fates of all ions are monitored. Note the breaks in the time axis (no ions are observed in the regions omitted from the figure). Here, a higher concentration of bombesin than normal was used (250 μM in DHB) to suppress signal from the matrix ions (DHB), which would otherwise saturate the detector: Trapping rf amplitude, V_1 = 400 Da, cooling rf amplitude, V_2 = 150 Da, cooling time 5 ms. Trapped ions were resonantly ejected with a mass extension ratio of 20.

were produced from a matrix of DHB. Peaks are apparent in the two different time regions. In the short time region (<0.1 ms), the peak at 30 μs arises from DHB ions and that at 80 μs from bombesin ions. Control experiments carried out with neat DHB and dyes confirmed the identity of the peaks in Figure 2. In the long time region (>30 ms), the group of peaks arises from peptide ions that are effectively trapped and subsequently ejected by resonant ejection. Comparison of the integrated intensity of trapped peptide ions, I_{trap}, versus that of untrapped peptide ions, I_{untrap}, provides a direct measure of the trapping efficiency from the same laser shot as given by the expression

$$\text{trapping efficiency} = 2I_{trap}/(2I_{trap} + I_{untrap})$$

where the factor of 2 arises because only half of the ion intensity is registered for resonantly ejected peptide ions. Losses that may occur on opaque regions of the end caps are not included in the present estimate of the ion trapping efficiency. However we note that simulations of the ion trajectories indicated that such losses are likely to be small.

The approach outlined above was used to systematically examine parameters that effect trapping efficiency, including the trapping rf (V_1), cooling rf (V_2), cooling time, ion acceleration potential, ion focusing potential, laser delay, and He gas pressure. We have found that high trapping efficiencies (in the m/z range of 500–8500) can readily be achieved by adjusting just three of these parameters (i.e., V_1, V_2, and laser delay) while keeping the other parameters constant (acceleration potential 25 V, focusing potential −150 V, and He pressure 1 mTorr). A summary of the

Table 1. Summary of Trapping Efficiency Measurements for Bombesin Ions Using Matched Dynamic Trapping, Dynamic Trapping, and Static Trapping[a]

trapping rf (V_1) (Da)[b]	cooling rf (V_2) (Da)[b]	laser delay (μs)[c]	trapping effic	trapping mode
400	150	−10	0.21	matched dynamic trapping
400	150	10	0.27	matched dynamic trapping
400	150	30	0.22	matched dynamic trapping
400	*250*	*30*	*0.39*	*matched dynamic trapping*
645	150	10	0.07	matched dynamic trapping
400	*400*	*10*	*0.10*	*dynamic trapping*
200	*200*	*230*	*0.03*	*static trapping*

[a] The entries in italics indicate the parameters that yielded the best trapping efficiency for the three different trapping schemes. [b] Low mass exclusion limit specified by the Finnigan ITMS control software. [c] The laser delay is specified with respect to the turn-on time of the rf amplitude (i.e., the laser delay is 0 when the rf amplitude is 0). The ion injection energy was 25 eV.

results of our trapping efficiency measurements is given in Table 1. Absolute trapping efficiencies as high as 39% were obtained for matched dynamic trapping—a factor of 13 higher than the best that we obtained with static trapping and 4 higher than the best that we obtained with dynamic trapping.

We explain the improved efficiency with the following model. Ions are injected into the trap with sufficient kinetic energy (25 eV) to readily penetrate the potential barrier at its periphery when the amplitude of the rf field is low. After the ions are injected, the rf field continues to ramp rapidly to large amplitude to supply a deeper potential well for trapping ions within the trap. During this period of time, collisional damping removes some of the kinetic energy of the ions but not enough to collapse (cool) the ions to the center of the trap—ions continue to oscillate with large amplitude about the center of the trap. If the envelope of the rf field is further increased and held at a high level (as in conventional dynamic trapping, Figure 1b), the trapping volume will shrink (as the result of the increased rf field) and ions with positions that fall outside this trapping volume will be expelled. This expulsion will occur even for ions with relatively low kinetic energies—i.e., values of kinetic energy that would allow the ions to be easily trapped were they positioned closer to the center of the trap. If, instead of maintaining the rf field at a high level, we lower it as illustrated in Figure 1c, the trapping volume can be enlarged while still maintaining a sufficiently deep potential well for efficient trapping. Those ions that would have been lost due to the shrunk trapping volume can then be trapped. Collisional damping during this period of time removes additional kinetic energy and the ions eventually collapse toward the center of the trap.

The model described above was inspired by direct measurements of the fate of ions during trapping. As an example, Figure 3 shows the results of an experiment performed under the same conditions as those used to obtain Figure 2 except that the cooling rf (V_2) was lowered from 150 (low mass exclusion limit as defined by the Finnigan control software) to 100 Da. A new group of peaks appeared between 300 and 600 μs, originating from bombesin ions that are trapped but not cooled to the center of the trap. As the rf field is reduced to the lower level (V_2 = 100 Da), the trapping potential becomes sufficiently shallow for ions with large orbits to escape the trap. The time difference between the new peaks in Figure 3 is ~35 μs, in agreement with the time

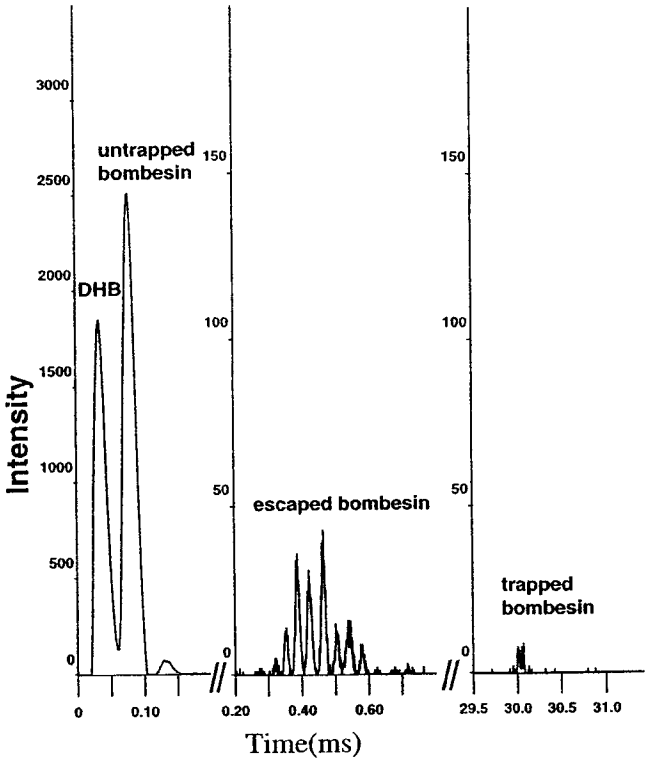

Figure 3. Trapping efficiency measurement as in Figure 2 with V_2 reduced from 150 to 100 Da.

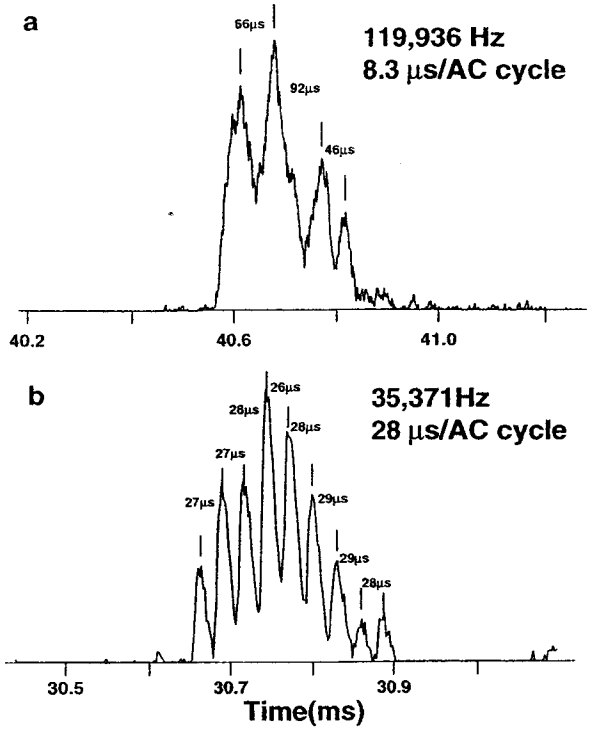

Figure 4. Temporal behavior of the resonantly ejected peptide ions with sequence HSDAVFTDNYTR (MM = 1425.5 Da) for different values of q_z and ac amplitude: (a) $q_z = 0.302$, ac amplitude 7.0 V_{p-p}; (b) $q_z = 0.0906$, ac amplitude 1.4 V_{p-p}.

required for the ions to circulate the trap as defined by the secular frequency of the bombesin ions. The time differences between adjacent peaks actually increase by ~1 μs/pair as a function of increasing time, reflecting the small decrease in secular frequency as the rf amplitude decreases. The existence of multiple peaks (a total of eight) suggests that ions are circulating with kinetic energies close to the changing trapping potential and that small decreases in the trapping potential allow additional ions to escape. This experiment demonstrates that even 600 μs after ions enter the trap, they are not cooled to its center but continue to orbit close to the boundary. For successful trapping, it is necessary to match both the kinetic energy of the ions with the trapping potential and the physical position of the ions with the trapping volume. These conditions are approximately achieved in matched dynamic trapping by carefully shaping the rf waveform. An additional benefit of matched dynamic trapping is its effect in lowering the internal energy of excitation of the trapped ions. Since the envelope of the rf amplitude is lowered during the trapping period, less internal energy is deposited via collisional activation. This is of practical importance for the use of MALDI because the MALDI process itself introduces considerable internal energy into the desorbed ion species.

No attempt was made to synchronize the firing of the laser with the phase of the driving rf potential. Such synchronization is unlikely to increase the trapping efficiency because ions that travel from the sample probe to the entrance end cap arrive with a considerable time spread (~20 μs for bombesin ions of 25 eV; see Figure 2). This time spread is long compared with the rf period (~1 μs) so that the injected ions will lose all phase relationship to the rf field during injection.

Resonant Ejection. Figure 4 compares the temporal behavior of ions when they are ejected at $q_z = 0.302$, $V_{p-p} = 7$ V, and mass extension ratio of 3 (Figure 4a) and $q_z = 0.0906$, $V_{p-p} = 1.4$ V, and mass extension ratio of 10 (Figure 4b). The ejection behavior under these two conditions is drastically different. In Figure 4a, the resonant ejection frequency is 119 936 Hz, corresponding to a period of 8.3 μs/ac cycle. Ions are not ejected during every ac cycle, but only every 6–11 ac cycles. Efficient ejection requires the use of a high ac amplitude because so few ac cycles satisfy the phase relationship for ejection. In contrast, when ions are ejected at lower q_z with a frequency of 35 371 Hz (corresponding to 28 μs/ac cycle), they are ejected during every ac cycle (Figure 4b). This observation suggests that at lower q_z the ejection phase relationship is satisfied within every ac cycle.

The results in Figure 4 can be understood by the following considerations. When the ejection frequency is lowered to give $\beta_z \approx 1/16$ (Figure 4b), the value of the ejection frequency drops to ~ 1/32 of the driving rf frequency—i.e., for every ac cycle there are 32 rf cycles. For a random initial phase difference between the ac and rf fields, the possibility of satisfying the ejection phase relationship is high—ions are ejected if any one of the 32 rf cycles satisfies the phase relationship. As the ejection frequency is increased to give $\beta_z \approx 1/5$ (Figure 4a), there are only 10 rf cycles for every ac cycle. The possibility of accidentally satisfying the ejection phase relationship is reduced and ejection does not occur on every ac cycle. It also appears that a much smaller ac ejection amplitude is needed if ions are ejected on every ac cycle (the low q_z case, Figure 4b) compared with the situation when ions are ejected on infrequent ac cycles (the high q_z case, Figure 4a).

The realization of efficient ejection at low q_z and low ac amplitude has a profound impact on the sensitivity and resolution of the ITMS. We show by the experiment illustrated in Figure 5 that the sensitivity is improved by almost 1 order of magnitude when ions are ejected at low q_z as compared with ejection at high q_z. Figure 5a shows the results obtained from a standard resonant

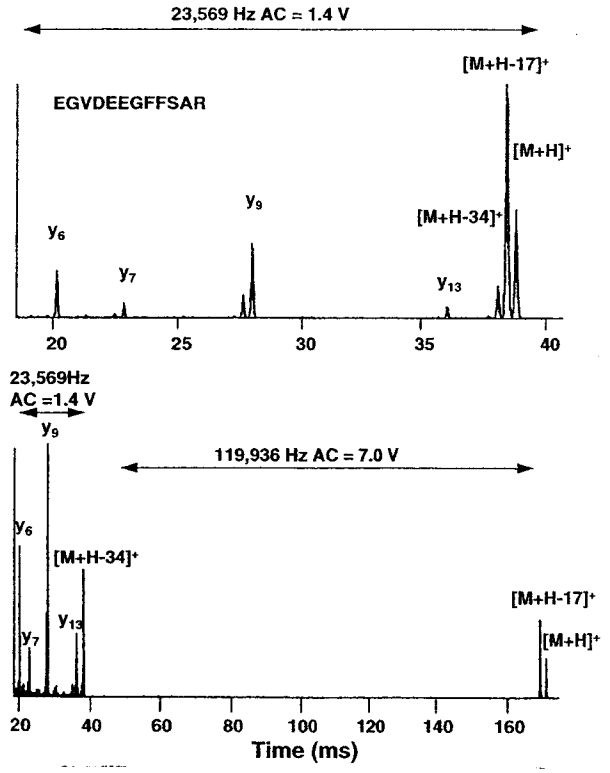

Figure 5. Demonstration of the improvement in ejection efficiency of protonated [Glu[1]]fibrinopeptide B at lower values of q_z and ac amplitude: (a, top) ejection at $q_z = 0.0604$ with an ac amplitude of 1.4 V_{p-p} (ejection frequency is 23 569 Hz); (b, bottom) same ejection conditions as in (a) for ions of y_6, y_7, y_9, y_{13}, and $[M + H - 34]^+$, but ejection at $q_z = 0.302$ with an ac amplitude of 7.0 V_{p-p} (ejection frequency is 119 936 Hz) for $[M + H - 17]^+$ and $[M + H]^+$ ions.

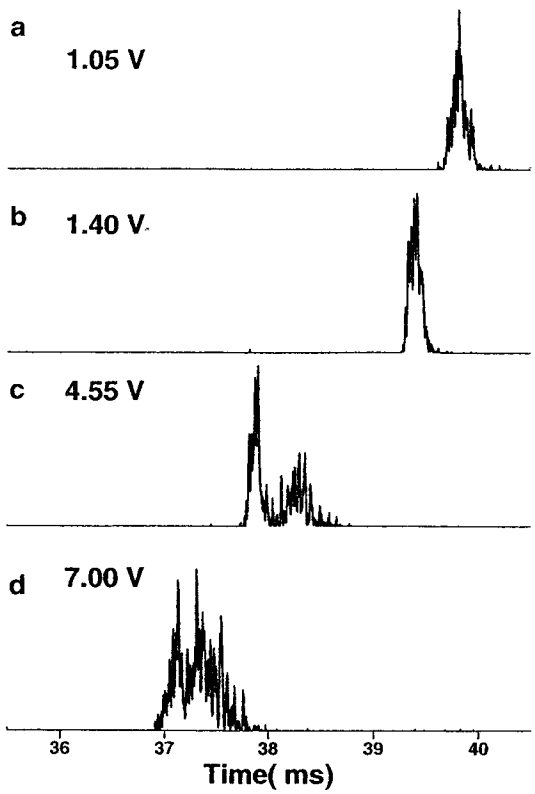

Figure 6. Peak shape of mass-isolated bombesin ions (4 u isolation window) as a function of the resonant ejection amplitude ($q_z = 0.0906$, ac frequency 35 371 Hz): (a) 1.05 V_{p-p}, (b) 1.40 V_{p-p}, (c) 4.55 V_{p-p}, and (d) 7.00 V_{p-p}.

ejection scan of the 13-residue peptide EGVDNEEGFFSAR, using an ac frequency of 23 560 Hz and an amplitude of 1.4 V_{p-p}—corresponding to a mass extension ratio of 15 ($q_z = 0.0604$). The spectrum exhibits peaks arising from the protonated peptide, $(M + H)^+$, as well as fragments arising from facile loss of NH_3 and cleavage adjacent to the acidic residues (y_6, y_7, y_9, and y_{13}).[17] The ratio (r_1) of intact $[M + H]^+$ ions to the y_6 fragment ions is 2.3. Figure 5b is an experiment that probes ejection of the same ions with two different frequencies. Masses up to $[M + H - 34]^+$ are ejected under the same conditions used to obtain Figure 5a (23 560 Hz, 1.4 V_{p-p}, mass extension ratio 15), while masses greater than $[M + H - 34]$ are ejected at 119 936 Hz, 7 V_{p-p}, mass extension ratio 3. While the early part of the scan shown in Figure 5b is essentially identical to that shown in Figure 5a, the intensities of $[M + H - 17]^+$ and $[M + H]^+$, which are ejected at high q_z, are much weaker than the same ions ejected at low q_z (Figure 5a). In Figure 5b, the ratio (r_2) of intact $[M + H]^+$ ions to y_6 fragment ions is 0.25. Thus, the absolute improvement in the response of the $(M + H)^+$ ions ejected at low q_z over those ejected at high q_z is $r_1/r_2 = 9.4$. This large improvement in response appears to be the consequence of the improved ejection efficiency at low q_z. As discussed above, a relatively low ac amplitude is needed to eject ions at low q_z. We shall see below that the use of low ac ejection amplitudes also leads to improved resolution.

It has been generally observed that the resolution of the ITMS degrades severely when the mass extension ratio is higher than 4.[9-12] We find that such severe resolution degradation only occurs when high ac ejection amplitudes are utilized (as in the conventional operation of the ion trap) and that we can obtain improved resolutions at mass extensions ratios as high as 10 by the use of low resonance ejection amplitudes (see below).

Figure 6 shows the effect of ejection amplitude on resolution for mass-isolated, intact protonated bombesin ions at a mass extension ratio of 10. At 1.05 V_{p-p}, the amplitude is too small to eject all the ions effectively (Figure 6a). Ejection becomes efficient upon increasing the amplitude to 1.4 V_{p-p} (Figure 6b), whereupon the resolution improves. However, further increases in ejection amplitude lead to drastically decreased resolution and complex peak shapes (Figure 6c,d).

Possible reasons for the complex peak shape include fragmentation during ejection by the supplemental ac field or early ejection due to interaction of the ions with higher-order components of the trapping field.[18,19] We tested the possibility of fragmentation during ejection by the experiment illustrated in Figure 7. The logic behind this experiment is that if the early peak in Figure 6c is due to fragmentation, then this fragmentation must occur at the moment of ejection or just prior to ejection. To test whether such fragmentation occurs, we stopped the rf ramp just prior to ejection of the early peak in Figure 6c, turned off the ac field (while maintaining the rf field) to cool any fragments that may have been formed, and then resonantly ejected all ions present in the trap. If fragmentation had occurred, the resulting fragments should be readily detected in this experiment.

(17) Qin, J.; Chait, B. T. *J. Am. Chem. Soc.* **1995**, *117*, 5411–5412.

(18) Williams, J. D.; Cox, K. A.; Cooks, R. G.; McLuckey, S. A.; Hart, K. J.; Goeringer, D. E. *Anal. Chem.* **1994**, *66*, 725–729.

(19) Wang, Y.; Franzen, J. *Int. J. Mass Spectrom. Ion Processes* **1994**, *132*, 155–172.

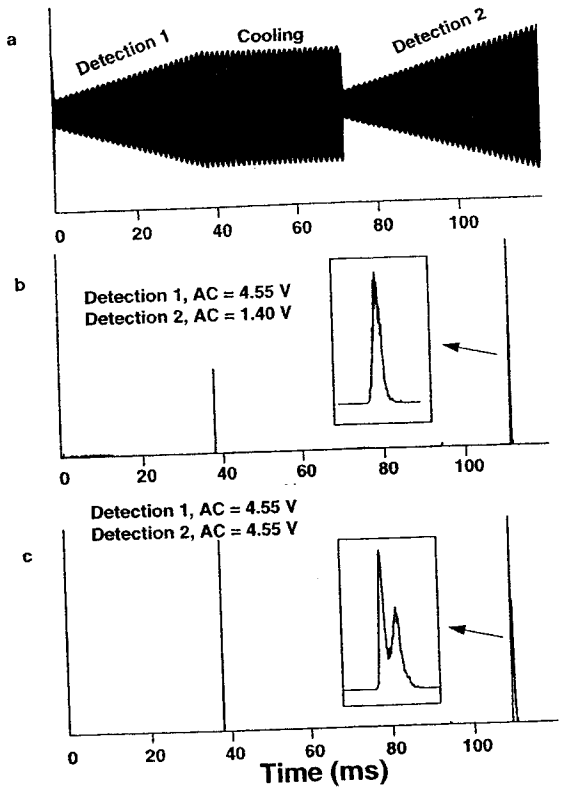

Figure 7. Demonstration that the complex peak shapes seen in Figure 6 are not due to dissociation during resonant ejection (see text). (a) The rf waveform used in the experiment. In detection stage 1, the rf amplitude is ramped to the point that mass-isolated bombesin ions just begin to be ejected. The ac frequency is 35 371 Hz and ac amplitude is 4.55 V_{p-p}. In detection stage 2, the rf amplitude is ramped to eject all ions in the trap with ac amplitude of either (b) 1.40 V_{p-p} or (c) 4.55 V_{p-p}. Insets show the peak shapes in detail.

Figure 7a shows the rf scan function used for the experiment. In the first rf detection scan, the amplitude is ramped to the point that a small portion of the early peak in Figure 6c is ejected using a high ac amplitude (4.55 V_{p-p}, 35 371 Hz). The front end of this early peak is seen as sharp peaks at 37.8 ms in Figure 7b,c. In the second rf detection scan, the amplitude is ramped over the full mass range to eject all ions present in the trap, but the ac amplitudes used for ejection are set to two different values, 1.4 (Figure 7b) and 4.55 V_{p-p} (Figure 7c). In Figure 7c, detection at the relatively high ac amplitude leads to a doublet which resembles the peaks shown in Figure 6c. By contrast, detection at low ac amplitude leads to a single peak (Figure 7b). We thus conclude that fragmentation during ejection by the supplemental ac field is not responsible for the complex peak shape.

The complex peak shape likely originates from the higher-order fields that are present in the stretched Finnigan ion trap.[18,19] Such higher-order fields may be exacerbated in our instrument since both end caps contain multiple holes (see Experimental Section). The existence of these higher-order fields has been experimentally demonstrated, and their effects have been shown to be increased at higher ac amplitudes.[18] The effect of these higher-order fields is to blue shift the secular frequency of the trapped ions, leading to early resonant ejection. The higher-order field effect is more prominent at lower values of q_z, where ions occupy space further from the center of the trap. The combination of a low q_z value and a high ac amplitude for resonant ejection accentuates effects of the higher-order fields that are not apparent at the high q_z values normally used for the detection of small ions.[3] This higher-order field effect appears to be the origin of the marked decline of resolution when mass extension ratios of >4 are used for resonant ejection at high ac amplitudes, and for the inability to assign masses accurately under these conditions.[9-12] With our improved understanding of ion trapping and ejection, we are now able to accurately measure peptides with m/z values up to 8.5 kDa with high sensitivity.[16]

CONCLUSION

A better understanding of the ion trapping process has lead us to devise an improved scheme for trapping, which we term matched dynamic trapping. We have also devised a means for directly measuring the trapping efficiency for peptide ions produced by MALDI. Our new trapping scheme yielded trapping efficiencies as high as 39%, which is a factor of 13 higher than that for static trapping and a factor of 4 higher than that for dynamic trapping. A better understanding of the resonant ejection process also led us to utilize low values of q_z and ac amplitude for ejection. This new resonant ejection parameter set increases the ejection efficiency by a factor of ~9 over more conventionally used parameter sets and allows for marked improvements in the mass resolution for ions with m/z > 2500. The combined improvements in the efficiencies of ion trapping and ejection together with inproved methods for ion isolation and fragmentation[7] lay the foundation for highly sensitive matrix-assisted laser desorption/ionization ion trap mass spectrometry.[16]

ACKNOWLEDGMENT

This work was supported in part by grants from the NIH (RR00862 and GM38724). The excellent technical assistance of Mr. Herbert Cohen is gratefully acknowledged. We thank Dr. Nathan Yates and Professor Richard Yost for supplying the ICMS control software and Drs. Hans Reiser and Randall Julian, Jr., and Professor Graham Cooks for supplying ITSIM.

Received for review November 29, 1995. Accepted March 29, 1996.[⊗]

AC951162U

[⊗] Abstract published in *Advance ACS Abstracts*, May 15, 1996.